IEEE Access
Multidisciplinary | Rapid Review | Open Access Journal

Received June 2, 2019, accepted June 29, 2019, date of publication July 16, 2019, date of current version August 7, 2019.

Digital Object Identifier 10.1109/ACCESS.2019.2929185

Compressive Sensing Based Spectrum Allocation and Power Control for NOMA HetNets

AHMED NASSER[1], OSAMU MUTA[2], MAHA ELSABROUTY[3], AND HARIS GACANIN[4]
[1]Graduate School of Information Science and Electrical Engineering, Kyushu University, Fukuoka 819-0395, Japan
[2]Center for Japan-Egypt Cooperation in Science and Technology, Kyushu University, Fukuoka 819-0395, Japan
[3]Department of Electronics and Communication, Egypt-Japan University of Science and Technology, Alexandria 21934, Egypt
[4]Nokia Bell Labs, 2018 Antwerp, Belgium

Corresponding author: Ahmed Nasser (ahmed.nasser@mobcom.ait.kyushu-u.ac.jp)

This work was financially supported and was done as a part of the research project Japan-Society-for-the-Promotion-of-Science (JSPS) KAKENHI under Grant JP17K06427. Also, this work was supported by the Center for Japan-Egypt Cooperation in Science and Technology, in part by Kyushu University, in part by the National Telecom Regulatory Authority (NTRA) (Super-HETs, Empowering 5G HetNets for better Performance), and in part by the Egyptian Ministry of Higher Education (MOHE).

ABSTRACT In this paper, a novel interference management technique based on compressive sensing (CS) theory is investigated for downlink non-orthogonal multiple access (NOMA) heterogeneous networks (HetNets). We mathematically formulate the interference management problem in terms of power and resource blocks (RBs) allocation to maximize the overall sum rate while considering both co-tier and cross-tier interferences and then explain its non-convexity. In this paper, we exploit the sparsity of the allocated RBs to relax the non-convexity of the formulated problem by transforming it into a sparse l_1-norm problem for a near-optimum solution. Then, based on the CS theory, an interference management technique with a restricted weighted fast iterative shrinkage-thresholding (R-WFISTA) algorithm is proposed to solve the equivalent sparse l_1-norm problem. The simulation results verify that compared with the conventional orthogonal multiple access (OMA) HetNets and conventional NOMA HetNets, the proposed technique improves the system performance in terms of overall sum rate and the outage probability.

INDEX TERMS Compressive sensing (CS), heterogeneous networks (HetNets), non-orthogonal multiple access (NOMA), power allocation (PA), sparsity.

I. INTRODUCTION

In the past years, heterogeneous networks (HetNets) are employed to improve coverage and sum rate of the cellular system by introducing overlapping tiers of small cells (SCs) that can co-exist in the coverage area of macro cell (MC) tier [1]. Recently, non-orthogonal multiple access (NOMA) technology is considered in HetNets to increase the overall sum rate in comparison with orthogonal multiple access (OMA) [2], [3]. In the widely adopted NOMA technique, namely, power-domain NOMA, users reuse the same resource blocks (RBs) via superimposed signals with different power levels. Thus, using NOMA introduces the challenge of managing the inter-user interference, which does not exist in OMA. In addition, the overlapping HetNets structure suffers from co-tier and cross-tier interference [4]–[7]. Thus, simultaneously managing all these types of interference is an urgent issue that needs to be considered to maintain the required performance level in NOMA HetNets.

The associate editor coordinating the review of this manuscript and approving it for publication was Walid Al-Hussaibi.

Regarding the inter-user interference, successive interference cancellation (SIC) is utilized at user side to recover the information iteratively from the superimposed signal [8]. On the other hand, one way to manage the co-tier and cross-tier interference in NOMA HetNets is to limit the number of BSs that share the same RBs [4]. Then, maximizing the system sum rate is achieved by jointly optimizing the allocated power and RBs to the deployed cells. However, the joint power and RBs allocation is NP-hard problem [5], [9]. In order to reduce the interference in HetNets, the system needs to efficiently allocate the RBs in time or frequency so that the same RB is sparsely reused among BSs in HetNets.

This paper proposes a novel interference management technique based on compressive sensing (CS) with the joint allocation of power and RBs in NOMA HetNets. We limit the number of BSs which reuse the same RB to meet the sparse allocation of RBs across the HetNets. The main contributions of this paper can be summarized as follows:

- We formulate the joint allocation of power and RBs problem to maximize the overall sum rate of NOMA HetNets while considering both co-tier and cross-tier interference. Since the formulated problem is non-convex, we relax the non-convexity by transforming the original problem into an equivalent sparse l_1-norm problem exploiting the sparsity of allocated RBs.

- Based on CS theory, we propose an interference management technique for NOMA HetNets with restricted weighted fast iterative shrinkage-thresholding (R-WFISTA) algorithm, where the power allocation to the BSs is restricted below a pre-determined upper bound.
- We theoretically analyze the optimum values for the power allocation coefficients, the outage probability and complexity of the proposed algorithm. Furthermore, the achievable performance in terms of system sum rate is compared with exhaustive search, conventional OMA HetNets, and conventional NOMA HetNets schemes.

The rest of the paper is organized as follows: Section II discusses the related works. Section III describes the mathematical signal model for NOMA HetNets and explains the problem formulation of the power and RBs allocation in NOMA HetNets. Section IV explains how to exploit the sparsity property of HetNets using CS to transform the original problem into a relaxed l_1-norm problem. Section IV also introduces the proposed R-WFISTA algorithm to solve the formulated l_1-norm problem. Section V investigates the theoretical performance of the proposed technique in terms of outage probability and computational complexity. Section VI simulates the performance of the proposed technique, while Section VII concludes the paper.

II. RELATED WORKS

Joint power and RB allocation problem has been considered in NOMA systems in terms of user clustering over different RBs and optimizing the power allocation coefficient as in [10], [11]. Authors in [10] propose a joint exhaustive search algorithm with a receive antenna selection scheme for a single cell uplink NOMA, while authors in [11] propose Lagrangian duality and dynamic programming algorithm for user clustering and power allocation to maximize the overall sum rate of single-cell NOMA systems taking only intra-user interference into account. Authors in [12] propose to use the KKT condition to find an optimal local solution for the power allocation problem in multi-cell NOMA, while considering a single RB is reused between cells to maximize the sum rate at the expense of increasing the co-tier interference between cells. However, the management of cross-tier interference due to the different cell size and transmission power in the HetNets scenario is not considered in the above works and a more challenging issue than single cell NOMA or homogeneous multi-cell NOMA scenarios, which needs a novel solution.

The power allocation problem has been considered in the HetNets systems to manage the induced cross-tier interference over the multi-cell scenario as in [5], [7], [13]–[17]. Authors in [5] propose a user scheduling scheme followed by a distributed power control algorithm to solve the PA problem. However, the algorithm in [5] considers HetNets with a single MC and one SC, and thus co-tier interference has not been taken into account. Authors in [14] propose that finding an optimal decoding order of NOMA users can help in solving PA problem in HetNets, while authors in [13] propose to employ coordinated multipoint (CoMP) with distributed power allocation scheme to manage the interference in NOMA HetNets. Authors in [15] propose a user clustering technique with a dual Lagrangian algorithm for power allocation in NOMA HetNets, while authors in [18] develop a mixed-integer programming framework for joint power allocation and user association in NOMA HetNets. Moreover, some works turned toward using the game theory to maximize the sum rate of NOMA HetNets systems by optimizing the allocated power to the BSs as in [7], [16], [17], where a non-cooperative game is proposed in [16], [17], while Stackelberg game is suggested in [7]. However, both [7], [16] consider only one small cell, and thus the co-tier interference has not been taken into account. Besides, the SBS is unfairly treated against the MBS in terms of sum rate due to the leader-follower role of the Stackelberg game. However, all the above works consider only the PA problem while maximizing the sum rate of HetNets by reusing the same RBs among all deployed BSs. Thus, the RB allocation problem over BSs in NOMA HetNets has not been taken into account. An efficient algorithm is needed to solve them jointly.

Some primary contributions have been made to find a sub-optimal solution for the joint problem of power and RBs allocation over BSs in NOMA HetNets as in [4], [6], [19]. Authors in [19] propose a dual-decomposition method for joint power and RB allocation in NOMA HetNets with non-ideal SIC receivers. However, in [19], BSs compete for different portions of the bandwidth, and thus the co-tier and the cross-tier interference have not been considered. Authors in [4], [6] apply matching theory to optimize the allocation of the power and RBs in NOMA HetNets, where multiple BS can reuse the same RBs. However, both [4], [6] optimize the allocated power to the SBSs only for maximizing the SCs sum rate, while the power allocated to the MBS is not considered. From these previous works, the general problem of maximizing the total sum rate of MC and SCs by allocating the RBs and fairly distributing the power among MBS and SBSs under the existence of both the co-tier and cross-tier interference has not been wholly considered, and more contributions need to be fulfilled.

III. NOMA HetNets

We consider a downlink NOMA HetNets, where N_{SC} SCs tiers of a single-antenna small BS (SBS) are adopted in the same coverage area of a single MC tier with a single-antenna macro BS (MBS). The MBS and each SBS serve, respectively, single-antenna N_{MU} macro-cell users (MUs) and $N_{SU} = 2$ small-cell users (SUs) via the NOMA scheme. The MC and the underlying SCs can reuse the same set of N_{RB} RB. Further, to limit the inter-user interference within the MC, we assume that the MUs are divided into K_m clusters, i.e., $K_m \leq N_{RB}$, each cluster has $N_{k_m} = 2$ MUs and reuses

TABLE 1. Definition of notations.

Notation	definition
$\boldsymbol{x}$, $\boldsymbol{X}$	Vectors and matrices are denoted with lowercase and uppercase boldface letters.
$\mathcal{SC}$, $\mathcal{RB}$	The set of SCs and RBs.
$\mathcal{MU}$, $\mathcal{SU}$	The sets of MC's users and SC's users.
N_{SC}, N_{RB}	Number of SC, and number of RBs.
N_{MU}, N_{SU}	Number of MUs in the MC, and SUs per SC.
$\mathrm{MU}_{k,n}$, $\mathrm{SU}_{i,n}$	The n^{th} user in the MC and i^{th} SC.
$\alpha^{[M_b]}$, $\alpha^{[S_b]}$	PA coefficients superscript M and S denote MC and SC, respectively.
$\#(.)$, $(.)^T$, $(.)^H$	Cardinality, transpose, and conjugate transpose operators.
$\|\cdot\|_f$, $\|\cdot\|_1$, $\|\cdot\|_2$	Frobenius norm, l_1 norm, and l_2 norm operators.
$\lvert . \rvert$, $\mathbb{C}^{a\times b}$	Absolute operator, and the complex matrix field of dimension $a \times b$.
$supp(\boldsymbol{a})$	Extracting the non-zero indices in the vector $\boldsymbol{a}$.
a\b, a⊥ b	Excluding 'b' from 'a', and 'a' is perpendicular to 'b'.

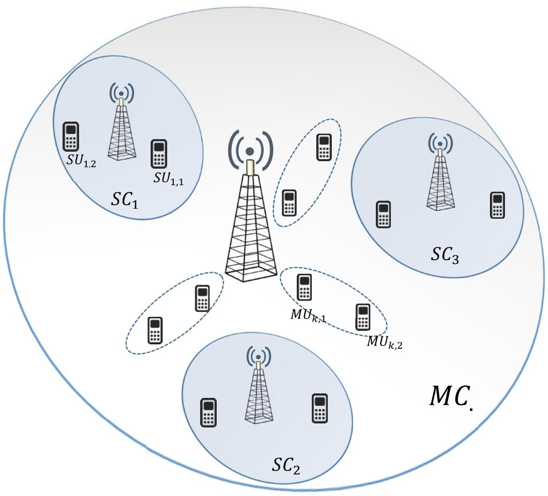

FIGURE 1. Illustration of the proposed HetNets model.

no more than one RB. Also, to limit the co-tier interference between SCs, we assume that each SC reuses no more than one RB, and an upper bound of q_{max} SCs can occupy the same RB.

A. MATHEMATICAL SIGNAL MODELLING

For NOMA signal detection using SIC,[1] we assume that the signals with worse channel conditions are decoded first and then respectively subtracted from the received superimposed signal [7], [20]. However, for fairness, the power allocated to the users within the SCs is inversely proportional to their channel condition. Also, we assume that each BS shares the users' CSI with a central control unit (CCU) through a high-speed backhaul link, and then CCU allocates RBs and power to BSs, while users are pre-associated to their appropriate MC or SCs.

[1] In this work, we assume that a perfect SIC detection is achieved at the receiver sides, which provides an upper bound in terms of the achieved data rates.

Let us consider $x_k^{[M_b]} = \sum_{n=1}^{N_{km}} \alpha_{k,n}^{[M_b]} p^{[M_b]} s_{n,k}^{[M_b]}$ and $x_i^{[S_b]} = \sum_{n=1}^{N_{SU}} \alpha_{i,n}^{[S_b]} p_i^{[S_b]} s_{i,n}^{[S_b]}$ are, consecutively, the transmitted superimposed signal from the MBS to its k^{th} cluster and that transmitted from i^{th} SBS to its SUs at the b^{th} RB. $p^{[M_b]}$ and $p_i^{[S_b]}$ are the transmitted powers from MBS and i^{th} SBS at b^{th} RB, respectively, while $s_{k,n}^{[M_b]}$ and $s_{i,n}^{[S_b]}$ are the transmitted message signals to $\mathrm{MU}_{k,n}$ and $\mathrm{SU}_{i,n}$, respectively. $\alpha_{k,n}^{[M_b]}$ and $\alpha_{i,n}^{[S_b]}$ are the PA coefficients of $\mathrm{MU}_{k,n}$ and $\mathrm{SU}_{i,n}$, respectively.

By considering $i \in \mathcal{SC} \triangleq \{1,\ldots,N_{SC}\}$, $n \in \mathcal{SU} \triangleq \{1,\ldots,N_{SU}\}$, and $b \in \mathcal{RB} \triangleq \{1,\ldots,N_{RB}\}$, the received signal at the n^{th} SU in the i^{th} SC over the b^{th} RB, $y_{i,n}^{[S_b]}$, can be written as:

$$y_{i,n}^{[S_b]} = \underbrace{h_{i,n}^{[S_b]} x_{i,n}^{[S_b]}}_{\text{Desired signal}} + \underbrace{h_{i,n}^{[S_b]} \sum_{l=1,\, l\neq n}^{N_{SU}} x_{i,l}^{[S_b]}}_{\text{Inter-user interference}} + \underbrace{\sum_{j=1,\, j\neq i}^{N_{SC}} f_{j,i,n}^{[S_b]} x_j^{[S_b]}}_{\text{Co-tier interference}} + \underbrace{g_{i,n}^{[S_b]} \sum_{k=1}^{K_m} x_k^{[M_b]}}_{\text{Cross-tier interference}} + \underbrace{z_{i,n}^{[S_b]}}_{\text{Noise}}, \quad (1)$$

where $x_{i,n}^{[S_b]} = \alpha_{i,n}^{[S_b]} p_i^{[S_b]} s_{i,n}^{[S_b]}$ is the transmitted signal to the n^{th} SU in the i^{th} SC, $\mathrm{SU}_{i,n}$, over the b^{th} RB. The coefficients $h_{i,n}^{[S_b]}$, $f_{j,i,n}^{[S_b]}$, and $g_{i,n}^{[S_b]}$ are the channel coefficients between SBS_i and $\mathrm{SU}_{i,n}$, the channel coefficients between SBS_j and $\mathrm{SU}_{i,n}$, and the channel coefficients between MBS and $\mathrm{SU}_{i,n}$, respectively, at the b^{th} RB. $z_{i,n}^{[S_b]}$ is the additive white Gaussian noise (AWGN) at $\mathrm{SU}_{i,n}$ with variance σ^2.

Furthermore, by assuming $k \in \mathcal{KM} \triangleq \{1,\ldots,K_m\}$, $n \in \mathcal{NK}_m \triangleq \{1,\ldots,N_{k_m}\}$, and $b \in \mathcal{RB}$, the received signal at the n^{th} MU in the k^{th} MC cluster over the b^{th} RB, $y_{k,n}^{[M_b]}$, can be written as:

$$y_{k,n}^{[M_b]} = \underbrace{h_{k,n}^{[M_b]} x_{k,n}^{[M_b]}}_{\text{Desired signal}} + \underbrace{h_{k,n}^{[M_b]} \sum_{l=1,\, l\neq n}^{N_{km}} x_{k,l}^{[M_b]}}_{\text{Intra-cluster interference}} + \underbrace{\sum_{i=1}^{N_{SC}} g_{i,k,n}^{[M_b]} x_i^{[S_b]}}_{\text{Cross-tier interference}} + \underbrace{z_{k,n}^{[M_b]}}_{\text{Noise}}, \quad (2)$$

where $x_{k,n}^{[M_b]} = \alpha_{k,n}^{[M_b]} p^{[M_b]} s_{k,n}^{[M_b]}$ is the transmitted signal to the n^{th} MU in the k^{th} MC's cluster, $\mathrm{MU}_{k,n}$, over the b^{th} RB. The coefficients $h_{k,n}^{[M_b]}$, and $g_{i,k,n}^{[M_b]}$ are the channel coefficients between MBS and its $\mathrm{MU}_{k,n}$, and the channel coefficients between i^{th} SBS and $\mathrm{MU}_{k,n}$ at the b^{th} RB, respectively. $z_{k,n}^{[S_b]}$ is the AWGN at $\mathrm{MU}_{k,n}$. Fig. 2 summarizes the signal transmission and detection models for $\mathrm{SU}_{i,n}$ and $\mathrm{MU}_{k,n}$.

As the MC and the SCs reuse the same RBs, three distinct kinds of interference affect the performance of the proposed system as obvious from equations (1) and (2). The inter-user and the intra-cluster interference occur between users in the same cell and the same cluster due to the non-orthogonal multiplexing of NOMA. Each SU experiences cross-tier and

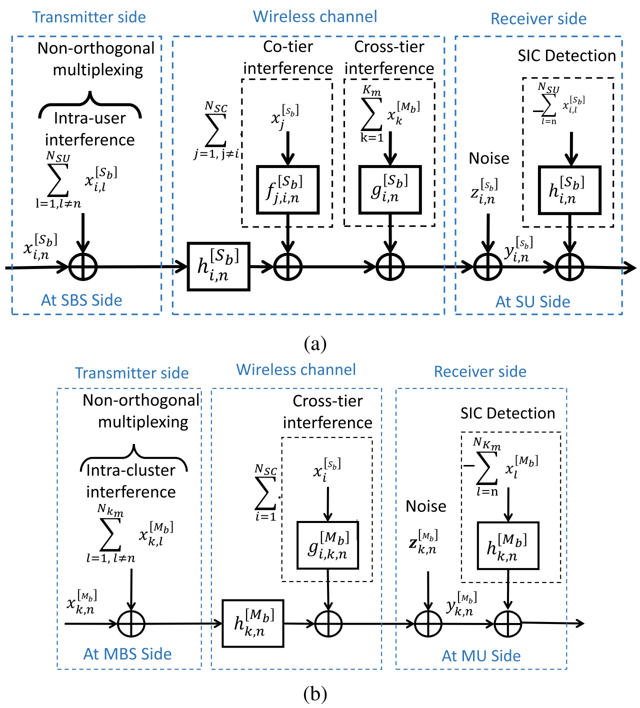

FIGURE 2. A block diagram for single-MC scenario that describes (a) the signal transmission and detection model for $SU_{i,n}$, and (b) the signal transmission and detection model for $MU_{k,n}$.

co-tier interference from MBS and SBSs that occupy the same RBs, respectively. Besides, MUs suffer a cross-tier interference from the SBSs that share the same RBs with the MBS.

B. PROBLEM FORMULATION

Unlike [4], [5], [7], we propose a general maximization problem of the total sum rate for MC and SCs by allocating the RBs while fairly distributing the power among MBS and SBSs at the presence of both the co-tier and cross-tier interference.

As described in [4], [5], the optimal decoding order of the NOMA users is performed in the ascending order of normalized channel gain. For SUs, the normalized channel gain is described as the channel gain-to-the noise, co-tier, and cross-tier interference. Consequently, the normalized channel gain for the $\mathrm{SU}_{i,n}$ at b^{th} RB, $\kappa_{i,n}^{[S_b]}$, can be expressed as:

$$\kappa_{i,n}^{[S_b]} = \frac{\left|h_{i,n}^{[S_b]}\right|^2}{\underbrace{\sum_{j=1, j\neq i}^{N_{SC}} \left|f_{j,i,n}^{[S_b]}\right|^2 P_j^{[S_b]}}_{\text{Co-tier interference}} + \underbrace{\left|g_{i,n}^{[S_b]}\right|^2 P^{[M_b]}}_{\text{Cross-tier interference}} + \sigma^2}, \tag{3}$$

To perform efficient SIC, the decoding order can be $\kappa_{i,1}^{[S_b]} \geq \kappa_{i,2}^{[S_b]} \geq \cdots \geq \kappa_{i,N_{SU}}^{[S_b]}$ for i^{th} SC. As described in [4], for the case that $N_{SU} = 2$, successful SIC at $\mathrm{SU}_{i,1}$ is guaranteed by

$$\Delta(\kappa_i^{S_b}) = \kappa_{i,1}^{[S_b]} - \kappa_{i,2}^{[S_b]} > 0 \tag{4}$$

Based on the normalized channel gain, $\kappa_{i,n}^{[S_b]}$, the signal to interference plus noise power ratio (SINR) for $\mathrm{SU}_{i,n}$ at b^{th} RB, $\gamma_{i,n}^{[S_b]}$, can be expressed by taking the inter-user interference into account as well as co-tier interference and cross-tier interference as

$$\gamma_{i,n}^{[S_b]} = \frac{\alpha_{i,n}^{[S_b]} P_i^{[S_b]} \kappa_{i,n}^{[S_b]}}{\sum_{l=1}^{n-1} \alpha_{i,l}^{[S_b]} P_i^{[S_b]} \kappa_{i,n}^{[S_b]} + 1}, \tag{5}$$

Similarly, as we assume a single MC scenario, the normalized channel gain is described as the channel gain-to-the noise and cross-tier interference. Consequently, the normalized channel gain for the $\mathrm{MU}_{k,n}$ at b^{th} RB, $\kappa_{k,n}^{[M_b]}$, can be expressed as:

$$\kappa_{k,n}^{[M_b]} = \frac{\left|h_{k,n}^{[M_b]}\right|^2}{\underbrace{\sum_{j=1}^{N_{SC}} \left|g_{j,k,n}^{[M_b]}\right|^2 P_j^{[S_b]}}_{\text{Cross-tier interference}} + \sigma^2}. \tag{6}$$

Similarly, the decoding order can be $\kappa_{k,1}^{[M_b]} \geq \kappa_{k,2}^{[M_b]} \geq \cdots \geq \kappa_{i,N_{k_m}}^{[M_b]}$ for k^{th} MC cluster. For $N_{k_m} = 2$, successful SIC at $\mathrm{MU}_{k,1}$ is guaranteed, as in [4], by

$$\Delta(\kappa_k^{M_b}) = \kappa_{k,1}^{[M_b]} - \kappa_{k,2}^{[M_b]} > 0 \tag{7}$$

By taking the intra-cluster interference as well as the cross-tier interference into consideration, the SINR for $\mathrm{MU}_{k,n}$ at b^{th} RB, $\gamma_{k,n}^{[M_b]}$, can be expressed as

$$\gamma_{k,n}^{[M_b]} = \frac{\alpha_{k,n}^{[M_b]} P^{[M_b]} \kappa_{k,n}^{[M_b]}}{\sum_{l=1}^{n-1} \alpha_{k,l}^{[M_b]} P^{[M_b]} \kappa_{k,n}^{[M_b]} + 1}. \tag{8}$$

Based on the SINR expressions in (5) and (8), the sum rates of all SCs and the MC at b^{th} RB can be determined by

$$\begin{aligned} R_{SCs}^{[b]} &= \sum_{i=1}^{N_{SC}} \sum_{n=1}^{N_{SU}} r_{i,n}^{[S_b]} \\ &= \sum_{i=1}^{N_{SC}} \sum_{n=1}^{N_{SU}} \log_2(1 + \gamma_{i,n}^{[S_b]}), \end{aligned} \tag{9}$$

and

$$\begin{aligned} R_{MC}^{[b]} &= \sum_{k=1}^{K_m} \sum_{n=1}^{N_{k_m}} r_{k,n}^{[M_b]} \\ &= \sum_{k=1}^{K_m} \sum_{n=1}^{N_{k_m}} \log_2(1 + \gamma_{k,n}^{[M_b]}), \end{aligned} \tag{10}$$

respectively, where $r_{i,n}^{[S_b]}$ and $r_{k,n}^{[M_b]}$ are the individual data rares for $\mathrm{SU}_{i,n}$ and $\mathrm{MU}_{k,n}$, respectively.

The proposed optimization problem aims to maximize the overall system sum rate, $R_{SCs}^{[b]} + R_{MC}^{[b]}$, by jointly optimizing the allocated RBs and powers to the MC and SCs under the constraints of interference existence. By assuming that the set of active SCs that simultaneously reuse the b^{th} RB is $\mathcal{SC}_b : \mathcal{SC}_b \subset \mathcal{SC}$, the proposed interference management optimization problem can be expressed as:

$$\max_{\mathcal{P}^{[b]}} R^{[b]}_{SCs} + R^{[b]}_{MC}, \tag{11}$$

$$s.t. \sum_{n=1}^{N_{km}} r^{[M_b]}_{k,n} \geq r^{[M_b]}_{th_k}, \quad \forall k, \tag{11a}$$

$$\sum_{n=1}^{N_{SU}} r^{[S_b]}_{i,n} \geq r^{[S_b]}_{th_i}, \quad \forall i, \tag{11b}$$

$$\#(\mathcal{SC}_b) \leq q_{max}, \quad \forall b, \tag{11c}$$

$$\mathcal{SC}_b \cap \mathcal{SC}_{b^*} = \phi, \quad \forall b^* \in \mathcal{RB} \setminus \{b\}, \tag{11d}$$

$$\Delta(\kappa_i^{S_b}) > 0, \ \Delta(\kappa_k^{M_b}) > 0 \quad \forall i, k, b, \tag{11e}$$

$$\mathcal{P}^{[b]} \leq \mathcal{P}^{[b]}_{max}, \tag{11f}$$

where the concatenated power vector $\mathcal{P}^{[b]} = [P_1^{[S_b]}, P_2^{[S_b]}, \ldots, P_{N_{SC}}^{[S_b]}, P^{[M_b]}]^T \in \mathbb{R}^{(N_{SC}+1)\times 1}$ contains the power of all SBSs and MBS at b^{th} RB, while $r^{[M_b]}_{th_k}$ and $r^{[S_b]}_{th_i}$ are the sum rates thresholds required for the k^{th} MC's cluster and i^{th} SC at b^{th} RB, respectively. The constraints (11a) and (11b) guarantee that the sum rates of SCs and the MC do not fall behind a predefined threshold $r^{[M_b]}_{th_k}$ and $r^{[S_b]}_{th_i}$, respectively. In (11a) and (11b), we utilize the sum rate of the cells instead of the individual data rates of the users as in (11) we allocate the power and RBs over BSs not over users. Constraint (11c) limits the number of SCs that can occupy the same RB by q_{max}, while the case that the number of BSs that reuse the same RBs is less than q_{max} possibly occurs if the allocated q_{max} BSs at a specific RB fail to satisfy the sum rate threshold constraints. The constraint (11d) is imposed to ensure that each SC reuses only one RB. The constraint (11e) ensures successful SIC at $\mathrm{SU}_{i,1}$ and $\mathrm{MU}_{k,1}$, while the constraint (11f) ensures that the allocated power to the MBS and SBSs do not exceed a certain maximum transmitting power at the b^{th} RB.

From the constraints (11a) and (11b), although the increase in the transmitted power from one of the BSs has a positive effect on the sum rate of its corresponding cell, it affects the other cells negatively through either cross-tier or co-tier interference. Consequently, it is difficult to determine the convexity of (11). Besides, from constraints (11c) and (11d), the RB allocation is a combinatorial problem of $\binom{N_{SC}}{q_{max}}$, which is a NP-hard problem. Thus, (11) is a non-convex combinatorial problem and, as far as we know, there is no systematic scheme that can find the optimum solution of this problem.

From another point of view, as a dedicated number of RBs are sparsely shared among all the BSs, the power vector, $\mathcal{P}^{[b]}$, can be considered sparse. In the following section, we reformulate (11) to l_1-norm convex problem based on the inherent sparsity property of $\mathcal{P}^{[b]}$ and solve it using the proposed CS approach. CS theory [11] emerges as a valuable tool that can recover a vector from far fewer measurements than conventional techniques once a suitable sparse representation exists [21].

IV. PROPOSED RESOURCE AND POWER ALLOCATION SCHEME BASED ON COMPRESSIVE SENSING

In HetNets, due to the insufficient number of available RBs compared to the number of the underlaid SBSs, i.e., $N_{RB} \ll N_{SC}$, a limited number of SBSs should be active in a dedicated RB. Thus, the power vector $\mathcal{P}^{[b]}$ can be adopted as a sparse vector with $q_{max}+1$ non-zero power values at the b^{th} RB as shown in Fig.3. We suggest that minimizing the sum of the BSs' power at dedicated RB is the best objective function in terms of convex functions to represent the allocation problem of power and RB, and is equivalent to the l_1-norm of the power vector $\mathcal{P}^{[b]}$.

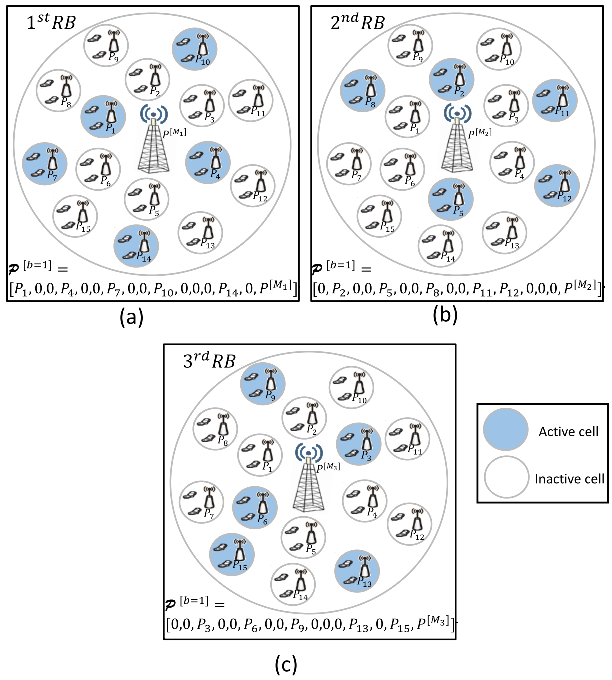

FIGURE 3. Illustrative examples of the HetNets sparsity property for the case of $N_{SC} = 15$, $N_{RB} = 3$, and $q_{max} = 5$. (a) Illustration of the RB allocation at 1^{st} RB, (b) illustration of the RB allocation at 2^{nd} RB, (c) illustration of the RB allocation at 3^{rd} RB.

Consequently, CS can be utilized to relax (7) to an equivalent convex l_1-norm problem to find a near-optimum solution for the sparse vector $\mathcal{P}^{[b]}$, $\forall b \in \mathcal{RB}$, as long as its two pillars, i.e., the dictionary matrix and the measurement vector, are properly designed. The dictionary matrix $\boldsymbol{\Psi}^{[b]} \in \mathbb{C}^{(N_{SC}+1)\times(N_{SC}+1)}$ acts as a linear sparsifying operator for $\mathcal{P}^{[b]}$. In this work, we design $\boldsymbol{\Psi}^{[b]}$ according to the co-channels among SBSs and the cross-channels between the MBS and SBSs. Later, we derive the compressed measurement vector, $\mathcal{I}^{[b]} \in \mathbb{C}^{K_q\times 1}$, $K_q << N_{SC}+1$. The measurement vector is designed in this work according to the allowable aggregated interference level on SCs and MCs.

A. DESIGN OF DICTIONARY MATRIX

To design the dictionary matrix at the b^{th} RB, $\boldsymbol{\Psi}^{[b]}$, we propose as in [5] to replace the non-linear constraints (11a) and

(11b) in (11) by the following equivalent linear form

$$\sum_{n=1}^{N_{km}} I_{k,n}^{[M_b]} \leq I_{th_k}^{[M_b]} \quad \forall k, \tag{12}$$

and

$$\sum_{n=1}^{N_{SU}} I_{i,n}^{[S_b]} \leq I_{th_i}^{[S_b]} \quad \forall i, \tag{13}$$

respectively, where $I_{k,n}^{[M_b]}$ and $I_{i,n}^{[S_b]}$ are the aggregated interference on $\mathrm{MU}_{k,n}$ and $\mathrm{SU}_{i,n}$ at b^{th} RB, respectively, while $I_{th}^{[M_b]}$ and $I_{th_i}^{[S_b]}$ are the maximum allowable aggregate interference on MC and i^{th} SC, respectively. The aggregated interference $I_{i,n}^{[S_b]}$ can be expressed as:

$$I_{i,n}^{[S_b]} = \left|h_{i,n}^{[S_b]}\right|^2 \sum_{k=n+1}^{N_{SU}} \alpha_{i,k}^{[S_b]} P_i^{[S_b]} + \sum_{j=1, j\neq i}^{N_{SC}} \left|f_{j,i,n}^{[S_b]}\right|^2 P_j^{[S_b]} + \left|g_{i,n}^{[S_b]}\right|^2 P^{[M_b]}. \tag{14}$$

Thus, the total interference on i^{th} SC, $I_i^{[S_b]}$, can be expressed as:

$$\begin{aligned} I_i^{[S_b]} &= \sum_{n=1}^{N_{SU}} I_{i,n}^{[S_b]} \\ &= \sum_{n=1}^{N_{SU}} \left|h_{i,n}^{[S_b]}\right|^2 \sum_{k=n+1}^{N_{SU}} \alpha_{i,k}^{[S_b]} P_i^{[S_b]} + \sum_{j=1, j\neq i}^{N_{SC}} \sum_{n=1}^{N_{SU}} \left|f_{j,i,n}^{[S_b]}\right|^2 P_j^{[S_b]} \\ &\quad + \sum_{n=1}^{N_{SU}} \left|g_{i,n}^{[S_b]}\right|^2 P^{[M_b]} \end{aligned} \tag{15}$$

For simplicity let $\beta_i^{[S_b]} = \sum_{n=1}^{N_{SU}} \left|h_{i,n}^{[S_b]}\right|^2 \sum_{k=n+1}^{N_{SU}} \alpha_{i,k}^{[S_b]}$, $\lambda_{j,i}^{[S_b]} = \sum_{n=1}^{N_{SU}} \left|f_{j,i,n}^{[S_b]}\right|^2$, and $\eta_i^{[S_b]} = \sum_{n=1}^{N_{SU}} \left|g_{i,n}^{[S_b]}\right|^2$. Consequently, equation (15) can be rewritten as

$$I_i^{[S_b]} = \beta_i^{[S_b]} P_i^{[S_b]} + \sum_{j=1, j\neq i}^{N_{SC}} \lambda_{j,i}^{[S_b]} P_j^{[S_b]} + \eta_i^{[S_b]} P_l^{[M_b]}. \tag{16}$$

Similarly, the total interference on the $\mathrm{MU}_{k,n}$, $I_{k,n}^{[M_b]}$, can be expressed as

$$I_{k,n}^{[M_b]} = \left|h_{k,n}^{[M_b]}\right|^2 \sum_{l=n+1}^{N_{km}} \alpha_{k,l}^{[M_b]} P^{[M_b]} + \sum_{j=1}^{N_{SC}} \left|g_{j,k,n}^{[M_b]}\right|^2 P_j^{[S_b]}, \tag{17}$$

Consequently, the total interference on the k^{th} MC's cluster, $I_k^{[M_b]}$, can be expressed as:

$$\begin{aligned} I_k^{[M_b]} &= \sum_{n=1}^{N_{km}} I_{k,n}^{[M_b]} \\ &= \sum_{n=1}^{N_{km}} \left|h_{k,n}^{[M_b]}\right|^2 \sum_{l=n+1}^{N_{km}} \alpha_{k,l}^{[M_b]} P^{[M_b]} + \sum_{j=1}^{N_{SC}} \sum_{n=1}^{N_{km}} \left|g_{j,k,n}^{[M_b]}\right|^2 P_j^{[S_b]}. \end{aligned} \tag{18}$$

For simplicity let $\beta^{[M_b]} = \sum_{n=1}^{N_{km}} \left|h_{k,n}^{[M_b]}\right|^2 \sum_{l=n+1}^{N_{km}} \alpha_{k,l}^{[M_b]}$, and $\eta_j^{[M_b]} = \sum_{n=1}^{N_{km}} \left|g_{j,k,n}^{[M_b]}\right|^2$. Consequently, equation (18) can be rewritten as

$$I_k^{[M_b]} = \beta^{[M_b]} P^{[M_b]} + \sum_{j=1}^{N_{SC}} \eta_j^{[M_b]} P_j^{[S_b]}. \tag{19}$$

Equations (16) and (19) can be combined in the following linear equation, $\forall i, k$, as

$$\boldsymbol{I}^{[b]} = \boldsymbol{\Psi}^{[b]} \boldsymbol{\mathcal{P}}^{[b]}, \tag{20}$$

where $\boldsymbol{I}^{[b]} = [I_1^{[S_b]}, I_2^{[S_b]}, \ldots, I_{N_{SC}}^{[S_b]}, I_k^{[M_b]}]^T \in \mathbb{C}^{(N_{SC}+1)\times 1}$ is the concatenated aggregate-interference vector over all SCs and the k^{th} active cluster of the MC at the b^{th} RB. The matrix $\boldsymbol{\Psi}^{[b]} \in \mathbb{C}^{(N_{SC}+1)\times(N_{SC}+1)}$ is the dictionary matrix at b^{th} RB. Equation (20) can be represented in a matrix from as

$$\begin{bmatrix} I_1^{[S_b]} \\ I_2^{[S_b]} \\ \vdots \\ I_{N_{SC}}^{[S_b]} \\ I^{[M_b]} \end{bmatrix} = \begin{bmatrix} \beta_1^{[S_b]} & \lambda_{2,1}^{[S_b]} & \lambda_{3,1}^{[S_b]} & \cdots & \lambda_{N_{SC},1}^{[S_b]} & \eta_1^{[S_b]} \\ \lambda_{1,2}^{[S_b]} & \beta_2^{[S_b]} & \lambda_{3,2}^{[S_b]} & \cdots & \lambda_{N_{SC},2}^{[S_b]} & \eta_2^{[S_b]} \\ \vdots & & \ddots & & & \vdots \\ \lambda_{1,N_{SC}}^{[S_b]} & \lambda_{2,N_{SC}}^{[S_b]} & \lambda_{3,N_{SC}}^{[S_b]} & \cdots & \beta_{N_{SC}}^{[S_b]} & \eta_{N_{SC}}^{[S_b]} \\ \eta_1^{[M_b]} & \eta_2^{[M_b]} & \eta_3^{[M_b]} & \cdots & \eta_{N_{SC}}^{[M_b]} & \beta^{[M_b]} \end{bmatrix} \begin{bmatrix} P_1^{[S_b]} \\ P_2^{[S_b]} \\ \vdots \\ P_{N_{SC}}^{[S_b]} \\ P^{[M_b]} \end{bmatrix}, \tag{21}$$

where proper constant values for the PA coefficients $\alpha_{k,n}^{[M_b]}$ and $\alpha_{i,n}^{[S_b]}$ can be used to determine $\boldsymbol{\Psi}^{[b]}$.

B. DESIGN OF MEASUREMENT VECTOR

To satisfy the constraints (12) and (13), the vector $\boldsymbol{I}^{[b]}$ in (20) must be replaced by the following interference threshold vector, $\boldsymbol{I}_{th}^{[b]} \in \mathbb{C}^{(N_{SC}+1)\times 1}$, as

$$\boldsymbol{I}_{th}^{[b]} = [I_{th_1}^{[S_b]}, I_{th_2}^{[S_b]}, \ldots, I_{th_{N_{SC}}}^{[S_b]}, I_{th_k}^{[M_b]}], \tag{22}$$

where $I_{th_i}^{[S_b]} = \sum_{n=1}^{N_{SU}} (|h_{i,n}^{[S_b]}|^2 \alpha_{i,n}^{[S_b]} P_{th_i}^{[S_b]})/(2^{r_{i,n}^{[S_b]}}-1)$ is the aggregated interference threshold on the $\mathrm{SU}_{i,n}$ at b^{th} RB and $P_{th_i}^{[S_b]}$ is the minimum required power for i^{th} SBS to achieve $r_{th_i}^{[S_b]}$, while $I_{th_k}^{[M_b]} = \sum_{n=1}^{N_{km}} (|h_{k,n}^{[M_b]}|^2 \alpha_{k,n}^{[M_b]} P_{th}^{[M_b]})/(2^{r_{k,n}^{[M_b]}}-1)$ is total interference threshold on $\mathrm{MU}_{k,n}$ at b^{th} RB and $P_{th}^{[M_b]}$ is the minimum required power for MBS to achieve $r_{th_k}^{[M_b]}$. Also, $I_{th_i}^{[S_b]}$ and $I_{th_k}^{[M_b]}$ can be empirically determined based on the system requirements. Thus, (20) can be rewritten as

$$\boldsymbol{I}_{th}^{[b]} = \boldsymbol{\Psi}^{[b]} \boldsymbol{\mathcal{P}}^{[b]} \tag{23}$$

According to the constraints (11c) and (11d), where no more than q_{max} SC can reuse the same RB, the power vector $\boldsymbol{\mathcal{P}}^{[b]}$ can be considered as a sparse vector with $q_{max}+1$ non-zero power values at the b^{th} resource block. To compensate this sparsity property of $\mathcal{P}^{[b]}$ and to put equation (23) into the form of CS, equation (23) must be multiplied by a compressed matrix $\boldsymbol{\Phi}$, where $\boldsymbol{\Phi}$ is a random matrix of dimension $K_q \times (N_{SC}+1)$ and $K_q \geq (q_{max}+1)log(N_{SC}+1)$. Consequently, equation (23) can be expressed as

$$\mathcal{I}^{[b]} = \boldsymbol{A}^{[b]} \mathcal{P}^{[b]} \tag{24}$$

where $\mathcal{I}^{[b]} = \boldsymbol{\Phi} \boldsymbol{I}_{th}^{[b]} \in \mathbb{C}^{k_q \times 1}$, and $\boldsymbol{A}^{[b]} = \boldsymbol{\Phi}\boldsymbol{\Psi}^{[b]} \in \mathbb{C}^{K_q \times (N_{SC}+1)}$ are the measurement vector and the sensing matrix at b^{th} RB, respectively. Consequently, the equivalent l_1-norm optimization problem to find the vector $\mathcal{P}^{[b]}$ can be formulated as

$$\begin{aligned} &\underset{\mathcal{P}^{[b]}}{\text{minimize}} \ \left\|\mathcal{P}^{[b]}\right\|_1 \\ &\text{subject to } \|\mathcal{I}^{[b]} - \boldsymbol{A}^{[b]}\mathcal{P}^{[b]}\|_2 \leq \epsilon, \end{aligned} \tag{25}$$

where ϵ is the error tolerance, and in this paper $\epsilon = 10^{-8}$ is used, while $\|\boldsymbol{x}\|_j = (\sum_{n=1}^{N}(x_n)^j)^{1/j}$ is the j^{th}-norm of a vector x. The resultant $\mathcal{P}^{[b]}$ is a $(q_{max}+1)$ sparse vector, which its non-zero indices represent the active BSs at the b^{th} RB, while the values of these indices denote the allocated power to these active BSs at b^{th} RB. To exploit $\mathcal{P}^{[b]}$ from (25), we propose R-WFISTA algorithm.

C. PROPOSED R-WFISTA ALGORITHM

To solve problem (25), a CS algorithm must be utilized. However, most CS algorithms use a threshold value to decide the non-zero coefficients with no upper bound on the maximum values of these coefficients [22], [23]. According to (11), an upper bound must be adopted to ensure that the allocated powers to the BSs do not exceed the maximum designed power. Also, the threshold value must be carefully chosen not to suppress the low-power tiers in HetNets. Thus, we propose a restricted WFISTA (R-WFISTA) algorithm as an extension for WFISTA proposed in [24], which is considered as a low-complex and fast convergence algorithm with an improved sparsity-undersampling trade-off. The proposed R-WFISTA algorithm is presented in step 1 of Algorithm 1. Two major modifications have been adopted to the proposed R-WFISTA algorithm that can be summarized as follow:

1) To satisfy the constraint (11f), an upper bound threshold function (denoted by $U_b(h)$ in step 1.4 in Algorithm 1) has been adopted to ensure that the estimated power vector does not exceed the maximum transmitting power threshold $\mathcal{P}^{[b]}{}_{max} = [P_{th_1}^{[S_b]}, P_{th_2}^{[S_b]}, \ldots, P_{N_{th_SC}}^{[S_b]}, P_{th}^{[M_b]}]$, where $P_{th_i}^{[S_b]}$ and $P_{th_i}^{[M_b]}$ denote the maximum transmitted power for the i^{th} SBS and the MBS, respectively.
2) The threshold value, τ, of the shrinkage function in the original WFISTA is estimated as a percentage of the maximum element in the empirical estimated sparse vector as $\tau = \eta \|\boldsymbol{A}^{[b]^H}\mathcal{I}\|_\infty$, where $\eta \in [.9 \ 1]$. However, as HetNets can deploy different tiers with different power levels (i.e., macro, micro, femto, and pico tiers), the above τ cannot be applied since the low-power tiers will not be allocated. In the proposed R-WFISTA, we adopt τ to be the minimum value of the $q_{max}+1$ maximum elements in the vector resulting from the summation of the updated vector and the residual error. In that case, the low-power tiers have more opportunity in power and RB allocation process. Step 1.6 in Algorithm 1 presents the proposed update of τ.

Algorithm 1 Proposed CS Scheme for Power and RB Allocation

– Initializing: $\mathcal{I} = \boldsymbol{\Phi}\boldsymbol{I}_{th}^{[1]}, \boldsymbol{A}^{[1]} = \boldsymbol{\Phi}\boldsymbol{\Psi}^{[1]}$, and $\Omega_r^{[1]} = \mathcal{SC}$
– For $b = 1$: RB
{
1. Estimating the sparse vector using WFISTA algorithm:
$\boldsymbol{q}$ = WFISTA $(\mathcal{I}^b, \boldsymbol{A}^{[b]})${
while $t < \mathcal{T}_{max}$ OR $\left\|f^t - f^{t-1}\right\|_2 > \epsilon$, repeat the following steps, where $\boldsymbol{h}^1 = \boldsymbol{0}$:
1.1 $\boldsymbol{q}^t = \eta_\tau(\boldsymbol{h}^t)$
1.2 $r^{t+1} = \dfrac{1+\sqrt{1+4r^t}}{2}$
1.3 $\boldsymbol{h}^{t+1} = \boldsymbol{q}^t + \dfrac{r^k - 1}{r^{k+1}}\eta_t(\boldsymbol{q}^t + \boldsymbol{W}_1\boldsymbol{q}^{t-1} + \boldsymbol{W}_2\boldsymbol{q}^{t-2}, \tau^t)$
1.4 Upper bounding $\boldsymbol{h}^{t+1}$
$$\boldsymbol{h}^{t+1} = U_b(\boldsymbol{h}^{t+1}) = \begin{cases} |h^{t+1}(m)| & |h^{t+1}(m)| \leq \mathcal{P}_{max}(m) \\ \mathcal{P}_{max}(m) & \text{Otherwise} \end{cases} \quad m \in \Omega_r^{[b]}$$
1.5 Ensuring SIC
if $\Delta(\kappa_i^{S_b}) < 0, \ \Delta(\kappa_k^{M_b}) < 0$
$\boldsymbol{h}^{t+1} = \boldsymbol{h}^t$
1.6 $f^{t+1} = \left\|\mathcal{I}^b - \boldsymbol{A}^{[b]}\boldsymbol{h}^{t+1}\right\|_2^2 + \lambda\left\|\boldsymbol{h}^{t+1}\right\|_1$
1.7 Updating threshold τ
$z^{t+1} = \mathcal{I}^b - \boldsymbol{A}^{[b]}\boldsymbol{h}^{t+1}$
$\boldsymbol{s} = \text{sort}(|\boldsymbol{h}^{t+1} + A^{[b]^H}z^{t+1}|, \text{descending})$
$\tau^{t+1} = \min(\boldsymbol{s})$
End while
2. Updating the power vector $\mathcal{P}^{[b]}$:
$\mathcal{P}^{[b]}(\Omega_r^{[b]}) = \boldsymbol{h}^t, \mathcal{P}^{[b]}(SC \setminus \Omega_r^{[b]}) = \boldsymbol{0}$
$\Omega^b = \text{supp}(\mathcal{P}^{[b]})$
3. Updating the sensing matrix $\boldsymbol{A}$ and the measurement vector $\mathcal{I}$
$\Omega_r^{[b+1]} = \Omega_r^{[b]} \setminus \Omega^{[b]}$
$\boldsymbol{A}^{[b+1]} = \boldsymbol{A}^{[1]}(\Omega_r^{[b+1]})$
$\mathcal{I}^{b+1} = \boldsymbol{\Phi}\boldsymbol{I}_{th}^{[1]}(\Omega_r^{[b+1]})$
}
– where:
sort($\boldsymbol{x}$, descending): sorts vector $\boldsymbol{x}$ in descending order.
min($\boldsymbol{x}$): finds the minimum value of the vector $\boldsymbol{x}$
$\eta_\tau(x, \tau) = \text{sign}(x)\max(0, |x| - \tau)$

In the proposed CS-PA-RB scheme presented in Algorithm 1, the proposed R-WFISTA estimates the sparse power vector at b^{th} RB, $\mathcal{P}^{[b]}$, by solving (25) in step 1. Then, the non-zero indices of the sparse vector that represent the active SCs at that RB are extracted using 'supp(x)' in step 2. In step 3, the measurement vector and the sensing matrix are updated by subtracting the estimated indices in step 2 from the remaining indices to estimate the sparse power vector at the next RB.

V. PERFORMANCE ANALYSIS

In this section, we investigate the theoretical performance of CS-PA-RB technique in terms of outage probability to discuss theoretical gains in comparison with conventional OMA and NOMA in HetNets. Later, we also compare the computational complexity in terms of the number of complex multiplications with respect to exhaustive search, swapping algorithm and the orthogonal matching pursuit (OMP).

A. OUTAGE PROBABILITY ANALYSIS

Guaranteeing a reliable communication without missing a fixed quality of service (QoS) threshold requires the SINR at users side not to fall below a threshold value. By applying our proposed technique in NOMA HetNets, the threshold on the SINR at the $SU_{i,n}$ over b^{th} RB can be expressed as:

$$\begin{aligned} \gamma_{i,n}^{[S_b]} &\geq \theta_{i,n}^{[S_b]} \\ \frac{\alpha_{i,n}^{[S_b]} P_i^{[S_b]} \kappa_{i,n}^{[S_b]}}{\sum_{l=1}^{n-1} \alpha_{i,l}^{[S_b]} P_i^{[S_b]} \kappa_{i,n}^{[S_b]} + 1} &\geq \theta_{i,n}^{[S_b]}, \end{aligned} \tag{26}$$

where $\gamma_{i,n}^{[S_b]}$ and $\theta_{i,n}^{[S_b]} = 2^{r_{i,n}^{[S_b]}} - 1$ are the SINR and its threshold value at $SU_{i,n}$ over the b^{th} RB. By optimizing the allocated power and RBs to the BSs using the proposed CP-PA-RB, the co-tier and cross-tier interference will be treated as a constant at SUs sides. Thus, the values of power allocation coefficients can be independently estimated for each SC directly from the individual QoS constraint (26) [20], [25]. By solving (26) for $n = 1, 2$ while $\alpha_{i,1}^{[S_b]} = 1 - \alpha_{i,2}^{[S_b]}$, the region for optimum values for $\alpha_{i,2}^{[S_b]}$ can be expressed as

$$\frac{\theta_{i,2}^{[S_b]}}{\left(1+\theta_{i,2}^{[S_b]}\right) \kappa_{i,2}^{[S_b]} P_i^{[S_b]}} \leq \alpha_{i,2}^{[S_b]} \leq \frac{\theta_{i,1}^{[S_b]}}{\kappa_{i,1}^{[S_b]} P_i^{[S_b]}}, \tag{27}$$

Since we have already optimized the BS's power, it is suitable to assume $\alpha_{i,1}^{[S_b]} + \alpha_{i,2}^{[S_b]} = 1$. The power allocation coefficients can be optimized by utilizing simple search algorithm over the region in (27) to maximize the individual data rate or by utilizing the difference-of-convex (DC) programming as in [15].

Further, the outage probability of $SU_{i,n}$ can be calculated as $\mathcal{P}out_{i,n}^{[S_b]} = \mathcal{P}r\left(\gamma_{i,n}^{[S_b]} < \theta_{i,n}^{[S_b]}\right)$, which can be further expressed for $SU_{i,1}$ and $SU_{i,2}$ as

$$\mathcal{P}out_{i,1}^{[S_b]} = \mathcal{P}r\left(\alpha_{i,2}^{[S_b]} > \frac{\theta_{i,1}^{[S_b]}}{\kappa_{i,1}^{[S_b]} P_i^{[S_b]}}\right). \tag{28}$$

$$\mathcal{P}out_{i,2}^{[S_b]} = \mathcal{P}r\left(\alpha_{i,2}^{[S_b]} < \frac{\theta_{i,2}^{[S_b]}}{\left(1+\theta_{i,2}^{[S_b]}\right) \kappa_{i,2}^{[S_b]} P_i^{[S_b]}}\right). \tag{29}$$

respectively. From the prove deduced in [20], the outage probabilities in (28) and (28) have an upper pound that can be expressed as

$$\mathcal{P}out_{i,n}^{[S_b]} \rightarrow \frac{1}{\rho_{i,n}^{[S_b]^{(N_{SU}-n+1)}}}, \tag{30}$$

where $\rho_{i,n}^{[S_b]}$ is the transmit signal to noise ratio for $SU_{i,n}$. In the same way, the threshold on the SINR at the MU_n can be formulated as:

$$\begin{aligned} \gamma_{k,n}^{[M_b]} &\geq \theta_{k,n}^{[M_b]} \\ \frac{\alpha_{k,n}^{[M_b]} P^{[M_b]} \kappa_{k,n}^{[M_b]}}{\sum_{l=1}^{n-1} \alpha_{k,l}^{[M_b]} P^{[M_b]} \kappa_{k,n}^{[M_b]} + 1} &\geq \theta_{k,n}^{[M_b]} \end{aligned} \tag{31}$$

where $\gamma_{k,n}^{[M_b]}$ and $\theta_{k,n}^{[M_b]} = 2^{r_n^{[M_b]}} - 1$ are the SINR and its threshold value at $MU_{k,n}$ over b^{th} RB. Similarly, the cross-tier interference can be treated as a constant at MUs sides. Thus, the feasible region power allocation coefficients can be independently estimated for each MC cluster by solving the individual QoS constraint (31) for $n = 1, 2$ and $\alpha_{i,1}^{[M_b]} = 1 - \alpha_{i,2}^{[M_b]}$ as

$$\frac{\theta_{k,2}^{[M_b]}}{\left(1+\theta_{k,2}^{[M_b]}\right) \kappa_{k,2}^{[M_b]} P^{[M_b]}} \leq \alpha_{k,2}^{[M_b]} \leq \frac{\theta_{k,1}^{[M_b]}}{\kappa_{k,1}^{[M_b]} P^{[M_b]}}, \tag{32}$$

Consequently, the outage probability at the $MU_{k,n}$, $\mathcal{P}out_{k,n}^{[M_b]}$, can be calculated as $\mathcal{P}out_{k,n}^{[M_b]} = \mathcal{P}r\left(\gamma_{k,n}^{[M_b]} < \theta_{k,n}^{[M_b]}\right)$ which can be further expressed for $MU_{k,1}$ and $MU_{k,2}$ as

$$\mathcal{P}out_{k,1}^{[M_b]} = \mathcal{P}r\left(\alpha_{k,2}^{[M_b]} > \frac{\theta_{k,1}^{[M_b]}}{\kappa_{k,1}^{[M_b]} P^{[M_b]}}\right). \tag{33}$$

$$\mathcal{P}out_{k,2}^{[M_b]} = \mathcal{P}r\left(\alpha_{k,2}^{[M_b]} < \frac{\theta_{k,2}^{[M_b]}}{\left(1+\theta_{k,2}^{[M_b]}\right) \kappa_{k,2}^{[M_b]} P^{[M_b]}}\right). \tag{34}$$

respectively. According to [20], the outage probabilities in (33) and (34) are upper bounded by

$$\mathcal{P}out_{k,n}^{[M_b]} \rightarrow \frac{1}{\rho_{k,n}^{[M_b]^{(N_{km}-n+1)}}}, \tag{35}$$

where $\rho_{k,n}^{[M_b]}$ is the transmit signal to noise ratio for $MU_{k,n}$.

B. COMPLEXITY ANALYSIS

The computational complexity of the proposed CS-PA-RB technique is determined by the complexity of the proposed R-WFISTA algorithm. At b^{th} RB, the overall computational complexity in terms of the number of complex multiplication of the proposed CS-PA-RB is upper bounded by $\mathcal{O}(K_q N_{SC})$, which comes from the matrix-vector multiplication part, $\boldsymbol{A}^{[b]}\boldsymbol{\mathcal{P}}^{[b]}$. The proposed R-WFISTA algorithm has the same complexity as the OMP algorithm [22], which represents the complexity benchmark for CS algorithms. Moreover, since the allocated q_{max} SBSs at b^{th} RB are subtracted from the

TABLE 2. The complexity order of the investigated algorithms.

Algorithm	Complexity
Exhaustive Search [26]	$\mathcal{O}((N_{SC})^{q_{max}})$
SOEMA [4]	$\mathcal{O}(N_{SC}N_{RB} + N_{SC}^2)$
opt-NOMA [12]	$\mathcal{O}(N_{SC}N_{SU}^2)$
Munkres Algorithm [19]	$\mathcal{O}(N_{SC}^3)$
WBM [19]	$\mathcal{O}(N_{SC}(K_m^3 + N_{MU}\, log\, N_{MU}))$
Proposed CS-PA-RB	$\mathcal{O}(K_q N_{SC})$

rest of SBSs in step 3.a of Algorithm 1, the computational complexity is reduced by q_{max} at every iteration over RBs. Thus, the computational complexity per iteration over RBs is estimated as $\mathcal{O}(K_q\langle N_{SC} - (b-1)q_{max}\rangle)$.

The bottleneck complexity order of different algorithm is listed in Table 2. It is obvious from Table 2 that the proposed algorithm has a much lower complexity compared to the complexity of the exhaustive search algorithm that increases exponentially with N_{SC} and q_{max}. Although the complexity of the proposed CS-PA-RB has the same order as the swap operations enabled matching algorithm (SOEMA) [4], the proposed CS-PA-RB provides lower complexity as $K_q < N_{SC}$. Also, in contrast with algorithms opt-NOMA [12] and weighted bipartite matching (WBM) [19], the complexity of the proposed scheme is independent of either the number of users per cell or the number of clusters.

TABLE 3. Simulation Parameters.

Parameter	Value
Maximum transmit power of MBS, $P_{max}^{[M]}$	46 dBm
Maximum transmit power of SBS, $P_{max}^{[S]}$	26 dBm
MC radius	500m
SC radius	50m
Noise Power	-174 dBm/Hz
Number of SCs, N_{SC}	from 9 to 40
Number of RBs, N_{RB}	5
Number of MUs, N_{MU}	20
Number of SUs per SC, N_{SU}	2
$d_{i,1}^{[S]}$	5 m to 25 m
$d_{i,2}^{[S]}$	25 m to 50 m
$d_{k,1}^{[M]}$	50 m to 200 m
$d_{k,2}^{[M]}$	200 m to 300 m
$d_{th}^{[S]}$	100 m
Free space path-loss exponent for MC and SC	3
Minimum data rates for SUs, $\{r_{i,1}^{[S_b]}, r_{i,2}^{[S_b]}\}$	{1, 0.5}
Minimum data rates for MUs, $\{r_{k,1}^{[M_b]}, r_{k,2}^{[M_b]}\}$	{2, 1}

VI. NUMERICAL RESULTS AND DISCUSSION

The assumed simulation parameters are given in Table 3. The SCs are assumed to be non-overlapped and adopted uniformly in the same coverage area of the MC with a minimum distance, $d_{th}^{[S]}$, between any two SCs. Each SC and MC's cluster reuse one RB and serve only two users simultaneously using NOMA, one is called cell-center user (i.e., $n = 1$) and the other is the cell-edge user (i.e., $n = 2$). The cell-center users are randomly picked from the ranges $d_{i,1}^{[S]}$ and $d_{k,1}^{[M]}$ far from their SBS and MBS, respectively, while the cell-edge users are randomly chosen from the ranges $d_{i,2}^{[S]}$ and $d_{k,2}^{[M]}$ far from their BSs. Moreover, SUs of all SCs are assumed to have the same minimum required data rates of $r_{i,n}^{[S_b]}$. Also, the minimum data rates required for MUs, $r_n^{[M_b]}$, are supposed to be equal among all MUs. Further, coefficients of the channel are generated by the product of the free space path, with the same exponent for SUs and MUs, and the Rayleigh fading with zero mean and unit variance as in [27].

The performance of the proposed technique[2] in terms of sum rate, outage probability, and fairness is compared to 1) conventional OMA HetNets [20], where the BS can serve at most one user with one RB, while each BS reuses different RB with maximum transmitting power; 2) conventional NOMA HetNets [20], where users within the cell are served using NOMA and each BS transmits maximum power over different RB; 3) exhaustive search [4], which is considered as a baseline for the optimal performance where RB and power allocation are obtained by the exhaustive search. The PA coefficients of the proposed and the compared techniques are chosen by applying the exhaustive search algorithm over the optimum ranges in (27) and (32).

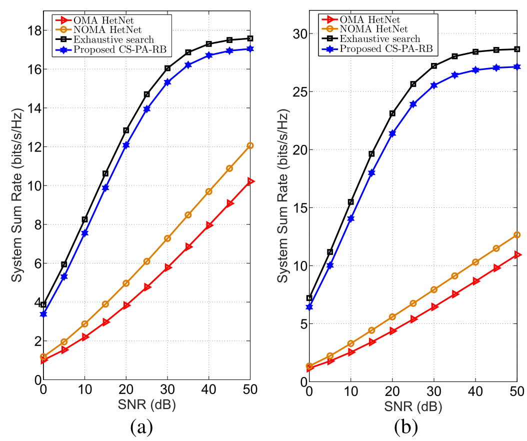

FIGURE 4. The performance of the proposed CS-PA-RB versus OMA HetNets [20] and NOMA HetNets [20] in terms of system sum rate at different values of SNR for (a) $N_{SC} = 9$ (b)$N_{SC} = 19$.

A. SUM RATE PERFORMANCE

Fig. 4 demonstrates the performance of the proposed CS-PA-RB technique in terms of the system sum rate, $\sum_{b=1}^{N_{RB}}(R_{MC}^{[b]} + R_{SCs}^{[b]})$, versus the averaged signal-to-noise ratio (SNR) among users for $N_{SC} = 9$ in Fig. 4(a), and $N_{SC} = 19$ in Fig. 4(b). It is clear from Fig. 4 that the

[2]MATLAB program is used in this section as a simulation tool to evaluate the performance of the proposed technique.

proposed CS-PA-RB provides system sum rate higher than conventional OMA and NOMA and close to the exhaustive search scheme, which indicates the efficiency of the proposed technique to manage the interference in HetNets. However, the growth rate of the proposed CS-PA-RB gets smaller as the SNR becomes higher since, at very high SNRs, the SINR depends mainly on the interference value.

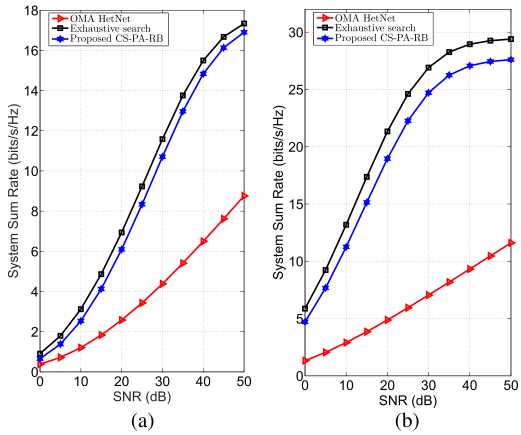

FIGURE 5. The performance of the proposed CS-PA-RB versus OMA HetNets [20] in terms of system sum rate at different values of SNR for $N_{SU} = 1$ and $N_{K_m} = 1$ in the case of (a) $N_{SC} = 9$ (b)$N_{SC} = 19$.

To validate the capability of the proposed algorithm in the case of OMA-HetNets, we simulate the system sum rate versus the SNR for $N_{SU} = 1$ and $N_{K_m} = 1$ in the case of $N_{SC} = 9$ in Fig. 5(a) and $N_{SC} = 19$ in Fig. 5(b). It is obvious that the proposed CS-PA-RB improved the performance of HetNets over conventional OMA even for $N_{SU} = 1$. This reflects the ability of CS-PA-RB to manage the interference due to reusing the same RB among the q_{max} SBSs in a better way than reusing one RB for each SBS with no interference in OMA.

Fig. 6(a) plots the system sum rate versus the number of SCs in the network, N_{SC}, for RB $= 5$. As can be noticed, the system sum rate of the proposed CS-PA-RB technique increases monotonically with N_{SC} since different SBSs simultaneously reuse the same RB. However, the sum rates in the conventional OMA and NOMA are restricted due to limited available RBs even when the number of SCs increases.

Fig. 6(b) shows the system sum rates of the proposed CS-PA-RB technique versus q_{max} at different numbers of N_{SC} for RB $= 5$. We can recognize that for a defined value of SBSs' number, N_{SC}, the sum rate of SCs rises to a fixed value as the q_{max} increases since RBs have been optimally allocated to all the SBSs after q_{max} reaches N_{SC}/RB. In particular, for the case of $N_{SC} = 20$, the SCs' sum rate saturates at $q_{max} > 4$. However, the increase rate becomes smaller with a larger value of q_{max} since increasing the number of SBS per RB will result in rising the cross-tier interference levels.

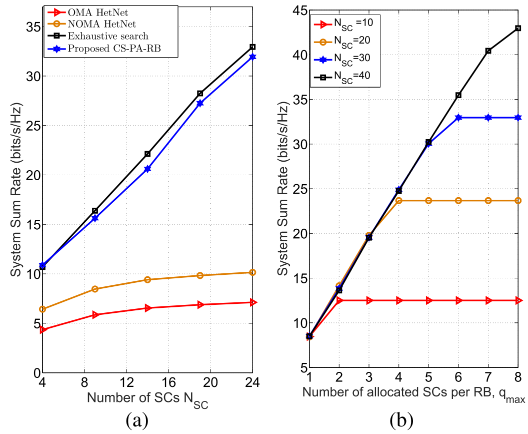

FIGURE 6. The performance of the proposed CS-PA-RB versus OMA HetNets [20] and NOMA HetNets [20] in terms of system sum rate at (a) different N_{SC} values (b) different q_{max} for different N_{SC}.

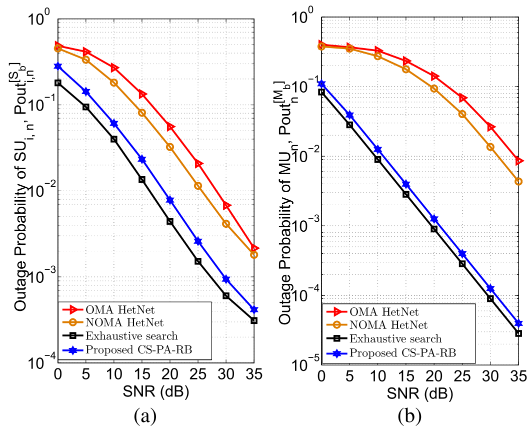

FIGURE 7. The performance of the proposed CS-PA-RB versus OMA HetNets [20] and NOMA HetNets [20] in terms of (a) outage probability of the $SU_{i,n}$, $\mathcal{P}out^{[S_b]}_{i,n}$ versus SNR, and(b) outage probability of the $MU_{k,n}$, $\mathcal{P}out^{[M_b]}_{k,n}$ versus SNR.

B. OUTAGE PROBABILITY AND FAIRNESS

At different levels of averaged SNR values, the performance of the proposed CS-PA-RB is evaluated in terms of outage probabilities of the $SU_{i,n}$ and $MU_{k,n}$ in Figs. 7(a) and 7(b), respectively. The outage probabilities of the $SU_{i,n}$ and MU_n are estimated by equations (28) and (33), respectively. It is obvious from Fig. 7 that outage probability of the proposed CS-PA-RB is lower than conventional OMA and NOMA techniques and very close to the outage probability of the exhaustive search technique. This is due to the ability of the proposed CS-PA-RB technique to manage the interference and provide higher SINR by using the CS theory to achieve near optimum allocation for power and RB even at low levels of SNR.

In addition, the outage probabilities of $SU_{i,n}$ and $MU_{k,n}$, are evaluated for wide ranges of the minimum required data rates, $r^{[S_b]}_{i,n}$ and $r^{[M_b]}_{k,n}$, in Figs. 8(a) and 8(b). The proposed

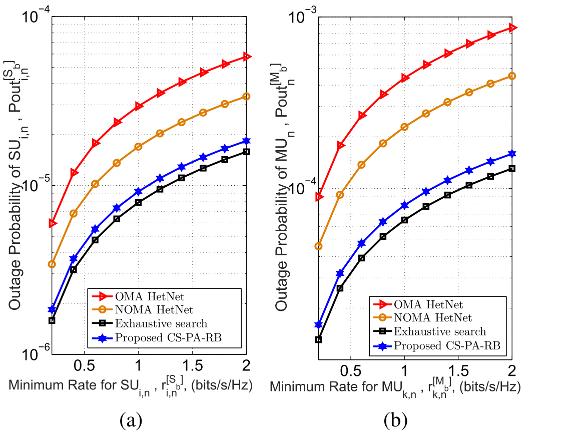

FIGURE 8. The performance of the proposed CS-PA-RB versus OMA HetNets [20] and NOMA HetNets [20] in terms of (a) outage probability of the $SU_{i,n}$, $\mathcal{P}out_{i,n}^{[S_b]}$, versus $r_{i,n}^{[S_b]}$, and (b) the outage probability of the $MU_{k,n}$, $\mathcal{P}out_{k,n}^{[M_b]}$, versus $r_{k,n}^{[M_b]}$.

CS-PA-RB gives lower outage probabilities than conventional techniques and close to the optimum values represented by the exhaustive search curve even for high required data rates. This means that CS-PA-RB technique can provide higher data rates for a given interference level than conventional techniques.

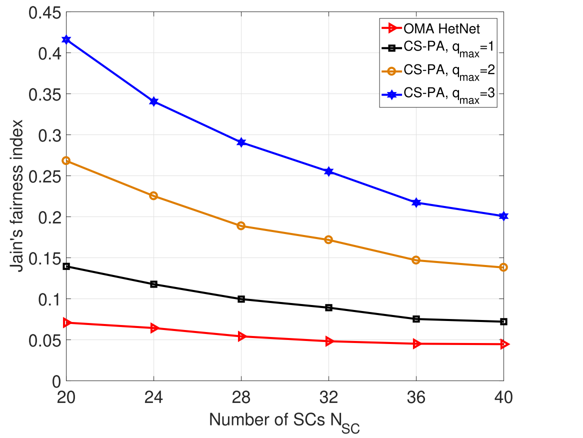

FIGURE 9. The Jain's fairness index versus the number of SCs, N_{SC}, for different q_{max} values.

Fig. 9 is plotted to assess the extent to which our proposed technique can fairly allocate the RBs among the BSs. Fig. 9 shows the RB allocation fairness of the proposed CS-PA-RB at different values of q_{max} versus the number of SCs, N_{SC}, compared to conventional OMA and NOMA (NOMA is equivalent to the case of the $q_{max} = 1$). In Fig. 9, we use the Jain's fairness index ($\mathcal{JF}$) [28] that can be determined by

$$\mathcal{JF} = \frac{(\sum_{i=1}^{N_{SC}} \sum_{n=1}^{N_{SU}} r_{i,n}^{[S_b]})^2}{2 \times N_{SC} \sum_{i=1}^{N_{SC}} \sum_{n=1}^{N_{SU}} (r_{i,n}^{[S_b]})^2} \tag{36}$$

and its range falls between 0 and 1, such that the Jain's fairness index of value equal to 1 indicates the fairest RB allocation where all users experience the same data rates. It can be observed that the fairness index of the proposed CS-PA-RB decay with the number of deployed SCs since any increase in the number of SCs above the value $RB \times q_{max}$ will result in more SCs that cannot access to the HetNets. Also, NOMA improves the fairness compared with OMA since, in NOMA, users have more opportunity to access the RBs as long as cell-center user and cell-edge user are properly paired. Moreover, as q_{max} gets larger, the number of SCs that can access the network will increase, which results in raising the fairness index.

VII. CONCLUSION

In this paper, the interference management problem in terms of optimizing the allocated power and RBs has been studied for HetNets. The NP-hard solving problem has been relaxed into an equivalent l_1 norm problem that can provide a near-optimum solution. A novel interference management algorithm, CS-PA-RB, has been proposed based on CS theory to solve the deduced equivalent l_1 norm using the R-WFISTA algorithm for a near-optimum power and RB allocation in HetNets. The improved performance of the proposed Cr-PA-RB algorithm in terms of system sum rate, outage probability, and fairness at various numbers of accommodated SCs and SNRs levels has been verified by the simulation results in comparison with conventional NOMA HetNets, OMA HetNets, and the exhaustive search.

REFERENCES

[1] V. Jungnickel, K. Manolakis, W. Zirwas, B. Panzner, V. Braun, M. Lossow, M. Sternad, R. Apelfrojd, and T. Svensson, "The role of small cells, coordinated multipoint, and massive MIMO in 5G," *IEEE Commun. Mag.*, vol. 52, no. 5, pp. 44–51, May 2014.
[2] Y. Saito, Y. Kishiyama, A. Benjebbour, T. Nakamura, A. Li, and K. Higuchi, "Non-orthogonal multiple access (NOMA) for cellular future radio access," in *Proc. IEEE 77th Veh. Technol. Conf. (VTC Spring)*, Jun. 2013, pp. 1–5.
[3] W. Shin, M. Vaezi, B. Lee, D. J. Love, J. Lee, and H. V. Poor, "Coordinated beamforming for multi-cell MIMO-NOMA," *IEEE Commun. Lett.*, vol. 21, no. 1, pp. 84–87, Jan. 2017.
[4] J. Zhao, Y. Liu, K. K. Chai, A. Nallanathan, Y. Chen, and Z. Han, "Spectrum allocation and power control for non-orthogonal multiple access in HetNets," *IEEE Trans. Wireless Commun.*, vol. 16, no. 9, pp. 5825–5837, Sep. 2017.
[5] D. Ni, L. Hao, Q. T. Tran, and X. Qian, "Power allocation for downlink NOMA heterogeneous networks," *IEEE Access*, vol. 6, pp. 26742–26752, 2018.
[6] Y. Gu, W. Saad, M. Bennis, M. Debbah, and Z. Han, "Matching theory for future wireless networks: Fundamentals and applications," *IEEE Commun. Mag.*, vol. 53, no. 5, pp. 52–59, May 2015.
[7] Z. Song, Q. Ni, and X. Sun, "Distributed power allocation for nonorthogonal multiple access heterogeneous networks," *IEEE Commun. Lett.*, vol. 22, no. 3, pp. 622–625, Mar. 2018.
[8] S. M. R. Islam, N. Avazov, O. A. Dobre, and K.-S. Kwak, "Power-domain non-orthogonal multiple access (NOMA) in 5G systems: Potentials and challenges," *IEEE Commun. Surveys Tuts.*, vol. 19, no. 2, pp. 721–742, 2nd Quart., 2017.
[9] M. S. Ali, H. Tabassum, and E. Hossain, "Dynamic user clustering and power allocation for uplink and downlink non-orthogonal multiple access (NOMA) systems," *IEEE Access*, vol. 4, pp. 6325–6343, 2016.
[10] W. A. Al-Hussaibi and F. H. Ali, "Efficient user clustering, receive antenna selection, and power allocation algorithms for massive MIMO-NOMA systems," *IEEE Access*, vol. 7, pp. 31865–31882, 2019.
[11] L. Lei, D. Yuan, C. K. Ho, and S. Sun, "Joint optimization of power and channel allocation with non-orthogonal multiple access for 5G cellular systems," in *Proc. Global Commun. Conf. (GLOBECOM)*, Dec. 2015, pp. 1–6.

[12] W. U. Khan, Z. Yu, S. Yu, G. A. S. Sidhu, and J. Liu, "Efficient power allocation in downlink multi-cell multi-user NOMA networks," *IET Commun.*, vol. 13, no. 4, pp. 396–402, Mar. 2018.
[13] M. S. Ali, E. Hossain, A. Al-Dweik, and D. I. Kim, "Downlink power allocation for CoMP-NOMA in multi-cell networks," *IEEE Trans. Commun.*, vol. 66, no. 9, pp. 3982–3998, Sep. 2018.
[14] L. Lei, E. Lagunas, S. Chatzinotas, and B. Ottersten, "NOMA aided interference management for full-duplex self-backhauling hetnets," *IEEE Commun. Lett.*, vol. 22, no. 8, pp. 1696–1699, Aug. 2018.
[15] S. Zhang, N. Zhang, G. Kang, and Z. Liu, "Energy and spectrum efficient power allocation with NOMA in downlink HetNets," *Phys. Commun.*, vol. 31, pp. 121–132, Dec. 2018.
[16] Y. Zhang, Y. Zhu, W. Xia, F. Shen, X. Zuo, F. Yan, and L. Shen, "Game-based power control for downlink non-orthogonal multiple access in HetNets," in *Proc. IEEE Global Commun. Conf. (GLOBECOM)*, Dec. 2018, pp. 206–212.
[17] A. Nasser, O. Muta, M. Elsabrouty, and H. Gacanin, "Interference mitigation and power allocation scheme for downlink MIMO-NOMA HetNet," *IEEE Trans. Veh. Technol.*, to be published.
[18] F. Nikjoo, A. Mirzaei, and A. Mohajer, "A novel approach to efficient resource allocation in NOMA heterogeneous networks: Multi-criteria green resource management," *Appl. Artif. Intell.*, vol. 32, nos. 7–8, pp. 583–612, 2018.
[19] A. Celik, M.-C. Tsai, R. M. Radaydeh, F. S. Al-Qahtani, and M.-S. Alouini, "Distributed cluster formation and power-bandwidth allocation for imperfect NOMA in DL-HetNets," *IEEE Trans. Commun.*, vol. 67, no. 2, pp. 1677–1692, Feb. 2019.
[20] Z. Ding, F. Adachi, and H. V. Poor, "The application of MIMO to non-orthogonal multiple access," *IEEE Trans. Wireless Commun.*, vol. 15, no. 1, pp. 537–552, Jan. 2016.
[21] E. J. Candès and M. B. Wakin, "An introduction to compressive sampling," *IEEE Signal Process. Mag.*, vol. 25, no. 2, pp. 21–30, Mar. 2008.
[22] J. A. Tropp, A. C. Gilbert, and M. J. Strauss, "Algorithms for simultaneous sparse approximation. Part I: Greedy pursuit," *Signal Process.*, vol. 86, no. 3, pp. 572–588, 2006.
[23] A. Beck and M. Teboulle, "A fast iterative shrinkage-thresholding algorithm for linear inverse problems," *SIAM J. Imag. Sci.*, vol. 2, no. 1, pp. 183–202, 2009.
[24] A. Nasser, M. Elsabrouty, and O. Muta, "Weighted fast iterative shrinkage thresholding for 3D massive MIMO channel estimation," in *Proc. IEEE 28th Annu. Int. Symp. Pers., Indoor, Mobile Radio Commun. (PIMRC)*, Oct. 2017, pp. 1–5.
[25] X. Chen, F.-K. Gong, G. Li, H. Zhang, and P. Song, "User pairing and pair scheduling in massive MIMO-NOMA systems," *IEEE Commun. Lett.*, vol. 22, no. 4, pp. 788–791, Apr. 2018.
[26] K. Lee, Y. Bresler, and M. Junge, "Subspace methods for joint sparse recovery," *IEEE Trans. Inf. Theory*, vol. 58, no. 6, pp. 3613–3641, Jun. 2012.
[27] S. Ali, E. Hossain, and D. I. Kim, "Non-orthogonal multiple access (NOMA) for downlink multiuser MIMO systems: User clustering, beamforming, and power allocation," *IEEE Access*, vol. 5, pp. 565–577, Mar. 2017.
[28] R. K. Jain, D.-M. W. Chiu, and W. R. Hawe, "A quantitative measure of fairness and discrimination," Eastern Res. Lab., Digit. Equip. Corp., Hudson, MA, USA, Tech. Rep. DEC-TR-301, 1984.

AHMED NASSER received the B.Sc. degree (Hons.) in electronics and communications engineering from Suez Canal University, Egypt, in 2012, and the M.Sc. degree in electronics and communications engineering from Egypt Japan University for Science and Technology, in 2016. He is currently pursuing the Ph.D. degree in electronics and communication with Kyushu University, Japan. He joined Suez Canal University as a Teaching Assistant. His research interests include interference mitigation in wireless networks, massive MIMO, heterogeneous networks, channel estimation, compressive sensing, and emerging technologies for 5G wireless communications.

OSAMU MUTA received the B.E. degree from Ehime University, in 1996, the M.E. degree from the Kyushu Institute of Technology, Japan, in 1998, and the Ph.D. degree from Kyushu University, in 2001. In 2001, he joined the Graduate School of Information Science and Electrical Engineering, Kyushu University, as an Assistant Professor, where he has been an Associate Professor with the Center for Japan-Egypt Cooperation in Science and Technology, since 2010. His current research interests include signal processing techniques for wireless communications and power-line communications, MIMO, and nonlinear distortion compensation techniques for high-power amplifiers. He is a Senior Member of IEICE. He received the 2005 Active Research Award from the IEICE Technical Committee of Radio Communication Systems and the 2014, 2015, and 2017 Chairman's Awards for excellent research from the IEICE Technical Committee of Communication Systems.

MAHA ELSABROUTY received the B.Sc. degree (Hons.) in electronics and electrical communication engineering from Cairo University, Egypt, and the M.Sc. and Ph.D. degrees in electrical engineering from the University of Ottawa. She is currently with Egypt-Japan University of Science and Technology (E-JUST). Her current research interests include massive MIMO techniques, interference management in HetNets, cognitive radio, intelligent techniques for wireless communications, and green communication systems.

HARIS GACANIN received the M.E. and Ph.D. degrees in EE from the Graduate School of Electrical Engineering, Tohoku University, Japan, in 2005 and 2008, respectively. Since April 2008 to May 2010, he has been, first, a Japan Society for Promotion of Science (JSPS) Postdoctoral Research Fellow and, then, an Assistant Professor with the Graduate School of Engineering, Tohoku University. He is currently with Nokia Bell Labs, Belgium. His research interest includes wireline and wireless communications with a focus on wireless network coding, channel estimation and equalization, cognitive radio, MIMO, wireless sensor networks, dynamic resource allocation, and iterative receivers. He is a Senior Member of IEICE. He was a recipient of the 2010 KDDI Foundation Research Grant Award and the 2008 JSPS Postdoctoral Fellowships for Foreign Researchers. He was the Chair of the IEICE Europe Section.